The average results from the three series of beam heights are shown in Table 3. It is evident that no matter what beam height is being tested, the inverse analysis furnishes the same results for the strain hardening properties of the ECC. This is a rather promising validation of the method since it excludes the possibility of structural influence on the material parameters determined. Finally, it is noted that the strain hardening properties, in terms of the value of ε_{t2}, obtained for the mix tested in the present project are lower than usually expected for ECC.

Table 3. Experimental results obtained through the inverse analysis. The results for each beam height represent the average of three experiments. The latter column gives the average and standard deviation for all nine beams.

h [mm]	40	50	60	Average	Std. dev.
E_{t1} [GPa]	34	33	34	33	7
E_{t2} [GPa]	0.30	0.20	0.21	0.24	0.06
f_{t1} [MPa]	2.5	2.5	2.6	2.6	0.2
f_{t2} [MPa]	4.3	4.0	4.1	4.1	0.3
ε_{t1} [$\mu\varepsilon$]	84	77	80	80	18
ε_{t2} [%]	0.6	0.8	0.7	0.7	0.1

8. CONCLUSIONS

This paper presents a new method for the inverse analysis of a ECC FPBT which proves able to distinguish between the strain hardening and the crack localization parts of the deflection, thus enabling the unambiguous extraction of the strain hardening properties. Compared with FEM, this method gives very precise results. The method also performs well in comparison with experiments. However, complementary UTT experiments are needed in order to finally validate the method.

ACKNOWLEDGEMENTS

The Knud Højgaard Foundation is gratefully acknowledged for supporting the work, while Kuraray Europe is credited for the generous delivery of the PVA fibers. Prof. V. C. Li and Assoc. Prof. H. Stang are also highly recognized for inspiring this work.

REFERENCES

[1] Li, V. C. 2003. On Eng. Cemen. Comp. (ECC). *J. Adv. Conc. Tech.*, (3), 215–230
[2] Hillerborg, A., Modéer, M. & Petersson, P. E. Analysis of crack formation and crack growth in concr. by means of frac. mech. and finite elements *Cem. Concr. Res.*, , 773–782
[3] Olesen, J. F. 2001. Fictitious Crack Prop. in Fiber-Reinf. Conc. Beams. *J. Eng. Mech.*, (3), 272–280
[4] Østergaard, L. 2003. Early-Age Frac. Mech. and Crac. of Conc. Dept. of Civil Eng., Tech. Univ. of Denmark

International RILEM Workshop on High Performance Fiber Reinforced
Cementitious Composites (HPFRCC) in Structural Applications
Honolulu, Hawai'i, 23-26 May 2005

POLYVINYL ALCOHOL FIBER REINFORCED ENGINEERED CEMENTITIOUS COMPOSITES: MATERIAL DESIGN AND PERFORMANCES

Shuxin Wang and Victor C. Li
Department of Civil and Environmental Engineering, University of Michigan, USA

Abstract

Polyvinyl alcohol (PVA) fiber is considered as one of the most suitable polymeric fibers to be used as the reinforcement of engineered cementitious composites (ECC), though the unique microstructure characteristics of PVA fiber add challenge to the material design. In this paper, the micromechanics based design procedure for a PVA-ECC suitable for structural applications is described, and practical design considerations including requirements on interface bond, matrix toughness, and flaw system are outlined for achieving balanced composite performances. The properties of an exemplary PVA-ECC design are summarized, including tensile behavior and compressive strength development, bending response, Young's modulus, autogenous and drying shrinkage, and freeze-thaw durability.

1. INTRODUCTION

Engineered Cementitious Composites (ECC) is a unique representative of the new generation of high performance fiber reinforced cementitious composites, featuring high ductility and medium fiber content. Material engineering of ECC is constructed on the paradigm of the relationships between material microstructures, processing, material properties, and performance, where micromechanics is highlighted as the unifying link between composite mechanical performance and material microstructure properties [1]. The established micromechanics models guide the tailoring of composite constituents including fiber, matrix and interface for overall performance, and elevate the material design from trial-and-error empirical testing to systematic holistic "engineered" combination of individual constituents. The microstructure to composite performance linkage can be further extended to the structural performance level and integrate the material design into performance based design concept for structures [2]. In that sense,

ECC embodies a material design approach in addition to being an advanced material and provides an additional degree of freedom in structural performance.

Polyvinyl alcohol (PVA) fiber emerged during a search of low cost high performance fibers for ECC. The hydrophilic nature of PVA fiber imposed great challenge in the composite design, as the fibers are apt to rupture instead of being pulled out because of the tendency for the fiber to bond strongly to cementitious matrix. Careful engineering in fiber geometry, fiber/matrix interface and matrix properties is of vital importance to achieve high ductility in PVA-ECC. To guide the tailoring process, micromechanical models accounting for the uniqueness of PVA-fiber were developed.

The objective of this paper is to provide a performance summary of an exemplary PVA-ECC. As large scale applications of ECC are emerging, the data collected here may serve as reference for structural engineers. To limit the paper length, the composite modeling and design considerations will be only briefly described.

2. COMPOSITE DESIGN GUIDELINE

The primary performance target in ECC design is tensile ductility. In addition, high strength and Young's modulus, tight crack width, and high durability are also preferred in general. In most applications, tensile strain capacity 2% is considered sufficient. In terms of strength, it is desirable if ECC compressive strength is comparable with regular high strength concrete. As to crack width, previous study [3] suggested that permeability would be in the same order of sound concrete when the crack width is below 80 -100 μm.

One dominant variable governing strength is water to binder ratio *w/cm*. Low *w/cm* is also beneficial to maintain mixture consistency and facilitate fiber distribution. As long as ductility is not compromised, low *w/cm* is desired in mix design. In this exemplary mix, *w/cm*=0.24 is used.

Tensile ductility may be gauged by the strain-hardening index J_b'/J_{tip}, where J_b' is the complementary energy of the fiber bridging stress vs. opening $\sigma(\delta)$ relation (as defined by Eqn. 1, where σ_0 is the peak bridging stress and δ_0 is the corresponding crack opening), and J_{tip} is the matrix toughness. $J_b'/J_{tip}>1$ is essential to achieve strain-hardening, and higher J_b'/J_{tip} leads to more saturated multiple cracking.

$$J_b' \equiv \sigma_o \delta_o - \int_0^{\delta_o} \sigma(\delta) d\delta \qquad (1)$$

Modeling of $\sigma(\delta)$ relation is one essential piece of ECC micromechanics, since it not only connects the fiber, matrix and interface properties to J_b' but also provides the estimation of maximum crack width before failure. Due to significant slip-hardening response during pullout, PVA-fiber may be pulled out from both sides across the crack, in contrast to one-way pullout typically observed in steel and other polymeric fibers. In addition, matrix spalling at the fiber exits has to be accounted for accurate estimation of crack opening. A complete model of $\sigma(\delta)$ relation for PVA-ECC can be found in [4]. In connection to J_b', a very strong interface bond leads to fiber rupture at small crack opening, resulting in small J_b'. On the other hand, a very weak interface may cause low

International RILEM Workshop on High Performance Fiber Reinforced Cementitious Composites (HPFRCC) in Structural Applications
Honolulu, Hawai'i, 23-26 May 2005

bridging strength and large crack opening. Parametric study indicates that to satisfy the crack width performance target (below 80 μm) the optimal interface properties should be in the range of 1.5 - 2.5 MPa for frictional stress and below 1.5 N/m for interface fracture energy, given adequate fiber diameter and length for easy fiber dispersion. Unfortunately, the bond properties of PVA fiber without any treatment are far above the optimal values.

Two approaches were adopted to reduce the excessive interface bond. On the fiber aspect, surface coating by oil was investigated. With increase of oiling content, both frictional stress and interface fracture energy decrease significantly. Consequently, J_b' increases with oiling content for a given matrix, as shown in Figure 1, where fiber volume fraction 2.0% was used. On the matrix aspect, fly ash was introduced. High volume fraction of fly ash tends to reduce both the interface bond and matrix toughness. Figure 2 shows effect of ASTM Type F fly ash content on J_b'/J_{tip}, where oiling content 1.2% was used for fiber and the fiber volume fraction was 2.0%. Besides, fly ash improves mixture workability and material sustainability. However, high content of fly ash leads to slower strength development at early age. It was found that fly ash to cement at 1.2 provided best overall performances, and this proportion is used in the following exemplary mix.

Equally as important as the interface bond tailoring is the matrix properties control. Matrix toughness below 12 N/m is preferred. Meanwhile, the matrix cracking strength must be limited not to exceed σ_0. Matrix flaw size distribution control may become necessary to ensure saturated multiple cracking. The determination of optimal flaw size can be found in [4]. However, if the matrix tensile strength without macro defects can be controlled to be below the variation range of σ_0, saturated multiple cracking will be guaranteed. For the optimal interface properties proposed above and PVA fiber volume fraction of 2.0%, the preferred matrix tensile strength without macro defects is 5.0 MPa.

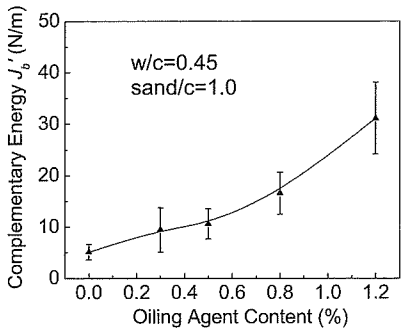

Figure 1: Effect of fiber surface oiling content on J_b'

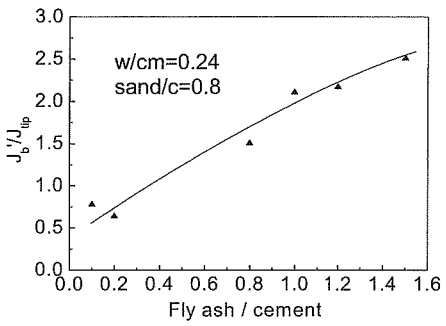

Figure 2: Effect of fly ash content on J_b'/J_{tip}

3. PVA-ECC PERFORMANCES

The mix proportions of the exemplary PVA-ECC (referred as M45) are given in Table 1. The volume fraction of fiber is 2%. ASTM Type I portland cement and low calcium ASTM class F fly ash were used. Large aggregates were excluded in ECC mix design, and only fine sand was incorporated. The silica sand used here had a maximum grain size of 250 μm and an average size of 110 μm. The PVA fiber had a diameter of 39 μm, a length of 12 mm, and overall Young's modulus of 25.8 MPa. The apparent fiber strength when embedded in cementitious matrix was 900 MPa. The fiber surface was treated with oil coating to reduce interface bond and the oiling content is 1.2%.

Table 1: Mix proportions of PVA-ECC (kg/m^3)

Cement	Sand	Class F Fly ash	Water	Superplasticizer	PVA Fiber
583	467	700	298	19	26

3.1 Tensile behavior

Tensile behavior was measured by direct uniaxial tension test. The coupon specimen measured 304.8 mm by 76.2 mm by 12.7 mm. Deformation was recorded with a gage length of 180 mm. Figure 3 shows the development of tensile strain capacity over age. The strain capacity at 24 hours after casting is about 2.3%. At early age, the strain capacity increases with time and reaches above 4% after 7 days, and later it decreases and then plateaus after about 30 days. The change in strain capacity reflects the evolutions of matrix toughness and interfacial bond properties. Figure 4 presents the typical tensile stress-strain curves after 24 hours and 90 days, where the tensile strength increases from 3.0 to 5.4 MPa.

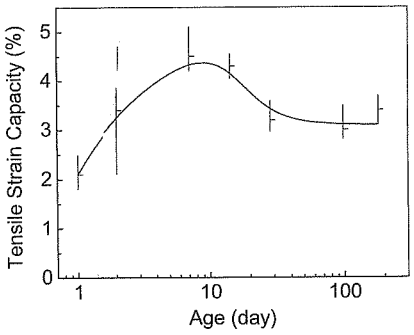

Figure 3: Age dependency of tensile strain capacity

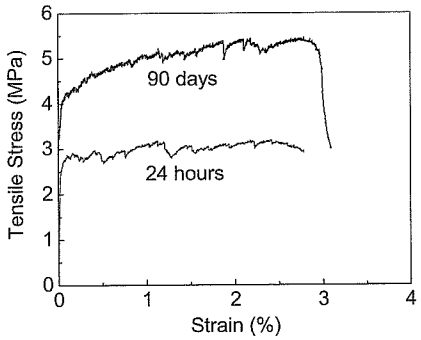

Figure 4: Typical tensile stress-strain curves at 24 hours and 90 days

Crack width in ECC prior to failure is limited by the crack opening corresponding to maximum bridging stress. Figure 5 shows the crack width development of PVA-ECC M45 at age of 28 days. The crack width remains under 60 μm until strain capacity is exhausted at 3.5%.

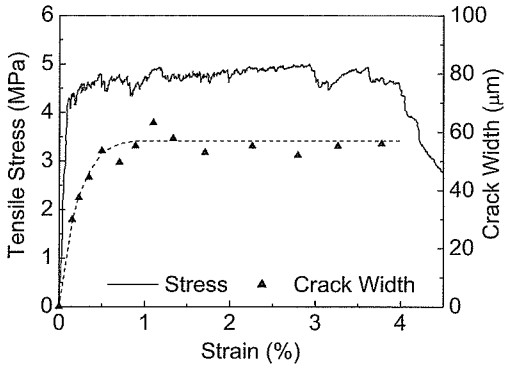

Figure 5: Crack width development

The robustness of tensile ductility may be enhanced by controlling pre-existing flaw size distribution in matrix [4], e.g. introduction of sufficient number of macro artificial flaws as crack initiators to ensure saturated multiple cracking. Figure 6 shows a set of tensile stress-strain curves of PVA-ECC M45 containing 7% by volume of polypropylene beads with 4 mm diameter. The age at test is 90 days. Consistent tensile performance with strain capacity exceeding 3% is demonstrated. Figure 7 shows the saturated multiple cracking pattern with average spacing less than 2 mm.

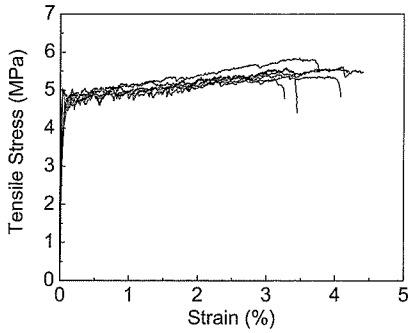

Figure 6: Robust tensile behavior of PVA-ECC with flaw size distribution control

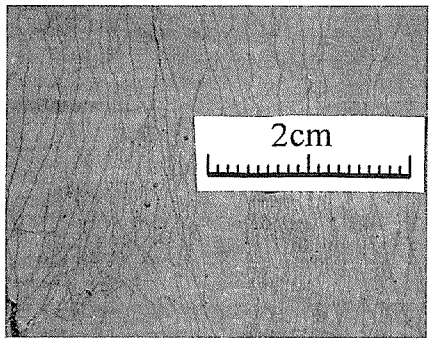

Figure 7: Multiple cracking pattern of PVA-ECC under uniaxial tension

3.2 Flexural behavior

Flexural response was measured by four point bending test. The beam specimen measures 304.8 mm (length) by 76.2 mm (width) by 25.4 mm (depth), and the bending

test span configuration is 101.6 mm by 76.2 mm by 101.6 mm. Figure 8 shows the typical flexural responses at 24 hours and 90 days. Significant deflection-hardening can be seen and the corresponding flexural strength is 11 and 16 MPa respectively. Figure 9 shows the cracking pattern of the tensile face at the constant moment section (90 days), and the average crack spacing is below 1.5 mm.

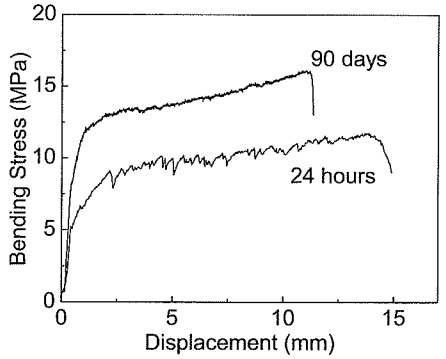

Figure 8: Flexural behavior of PVA-ECC

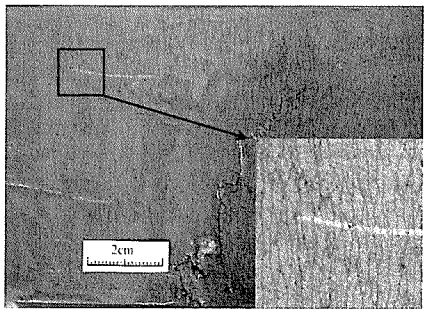

Figure 9: Multiple cracking pattern under bending

3.3 Compressive strength

Compressive strength was measured using 75 mm (diameter) by 150 mm (height) cylinders. Figure 10 shows the strength development of PVA-ECC M45 up to 8 months. Rapid strength gain was seen in the first 14 days and the 14 days strength is about 65 MPa. After that, the strength gain was much slower and at 8 months the strength is 75 MPa.

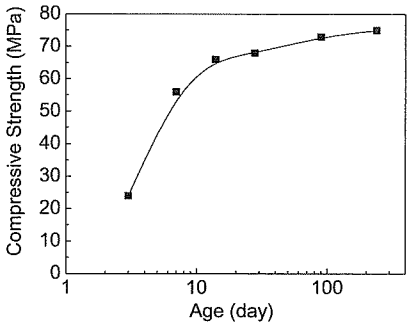

Figure 10: Compressive strength development

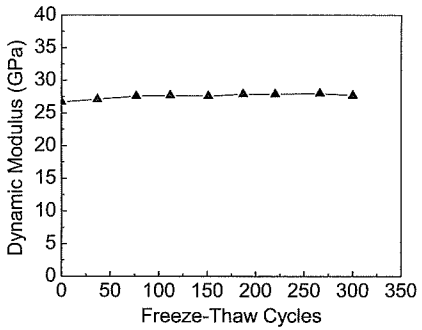

Figure 11: Freeze-thaw durability

International RILEM Workshop on High Performance Fiber Reinforced
Cementitious Composites (HPFRCC) in Structural Applications
Honolulu, Hawai'i, 23-26 May 2005

Similar to high strength concrete, PVA-ECC M45 exhibits nearly linear behavior under compression prior to failure. The Young's modulus is 20.4 MPa as measured at 28 days, and the peak stress reaches at 0.43% strain.

3.4 Freeze-thaw resistance

The test of freeze-thaw durability followed ASTM C666 Procedure A. The specimens were exposed to freeze-thaw cycles 14 days after casting. Figure 11 shows the dynamic modulus measured during 300 freeze-thaw cycles, and no deterioration was observed. After 300 cycles, the tensile strain capacity was recorded as 2.8 ± 0.6%, only slightly decreased from 3.0 ± 0.5% measured from specimens of the same age (14 weeks) not subjected to freeze-thaw condition. The compressive strength after 300 cycles was 60.7 ± 2.1 MPa, which was 22% lower than control specimens cured in room temperature.

3.5 Shrinkage behavior

Drying shrinkage was measured according to ASTM C157/C157M-99 and C596-01. The specimens were demolded after one day and stored in water for 2 days before they were moved to different relative humidity environments and the measurement was started. Free drying shrinkage deformation was monitored until hygral equilibrium was reached. Figure 12 shows the drying shrinkage of PVA-ECC M45 under various relative humidity. Due to the high binder content in ECC, the drying shrinkage of PVA-ECC M45 is about 80% higher than normal structural concrete.

Autogenous deformation is the bulk deformation of a closed, isothermal, cementitious material system not subjected to external forces [5]. Depending on material composition and hardening stage, it can be either expansion or shrinkage. The measurement of autogenous deformation of PVA-ECC M45 used dilatometer following Jensen and Hansen [6]. The mixture was cast under vibration into corrugated polyethylene tube with 25 mm diameter. The specimen length is approximately 300 mm. After casting, the specimen was placed in a dilatometer and immersed into constant temperature glycol bath. The change of specimen length was measured by displacement transducer. Before setting, the corrugated tube transforms the volumetric change into linear deformation, due to much higher stiffness in the radial than the longitudinal direction. Figure 13 shows the autogenous deformation immediately after casting up to 47 days, in which positive deformation is shrinkage. The zero deformation was defined at the moment of setting [7], which occurred at about 11 hours after casting. Rapid autogenous shrinkage was recorded in the first two days, mainly due to chemical shrinkage. Afterward, the development exhibits a plateau. It should be mentioned that the measurement of drying shrinkage (Figure 12) does not include the rapid deformation in the first 3 days.

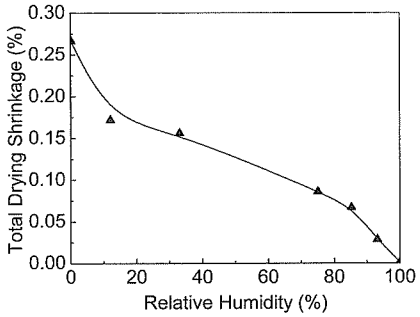

Figure 12: Drying shrinkage

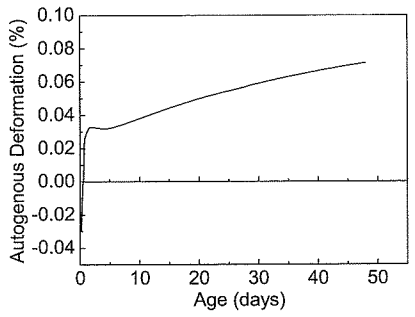

Figure 13: Autogenous shrinkage

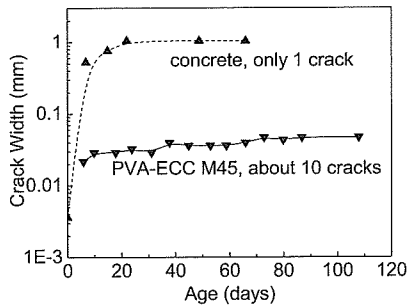

Figure 14: Crack width under restrained shrinkage

Although the drying shrinkage of PVA-ECC M45 is higher than normal concrete, it does not necessarily lead to large shrinkage crack width. Cracking behavior under restrained shrinkage was investigated using a ring test [8], where the deformation of concrete ring was restrained by a stiff steel tube inside. In this test, the diameter of the steel tube is 308 mm and the thickness is 18.5 mm. The ECC ring cast outside the steel tube has a thickness of 23 mm and a height of 150 mm. The specimen was sealed after casting and stored for 3 days. After that, the specimen was exposed to relative humidity of 50% at room temperature. The development of crack width and number at ring surface is shown in Figure 14, along with a concrete reference specimen. About 10 cracks were observed on the PVA-ECC M45 specimen and the crack width was below 50 μm. In contrast, only one large crack was developed in concrete, and the crack width is about 1 mm. Since the free shrinkage of M45 (<0.3 %) is far below the tensile strain capacity (Figure 3), the material undergoing restrained shrinkage is still in the strain-hardening stage. Hence the shrinkage crack width is a material property, implying that the shrinkage induced crack width of ECC is independent of structural dimension or reinforcement ratio [9].

4. CONCLUSIONS

- Micromechanics models have been proven a powerful tool in PVA-ECC design. Through interface and matrix tailoring, PVA-ECC delivers tensile strain capacity exceeding 3%, along with tensile strength > 5 MPa, flexural strength > 15 MPa, and compressive strength > 70 MPa.
- Crack width in PVA-ECC is a material property, and is controlled to below 60 μm. In addition, PVA-ECC exhibits excellent freeze-thaw durability.
- Although drying shrinkage of PVA-ECC is higher than structural concrete due to high binder content, the cracking behaviour under restraint shrinkage is much better than concrete due to strain-hardening.

International RILEM Workshop on High Performance Fiber Reinforced Cementitious Composites (HPFRCC) in Structural Applications
Honolulu, Hawai'i, 23-26 May 2005

ACKNOWLEDGEMENTS

The works reported here are supported by a series of grants to the University of Michigan by the National Science Foundation, Michigan Department of Transportation, and Kuraray Co., Japan. The authors would like to thank Mr. Mike Lepech, Dr. Pietro Lura, Dr. Ole Jensen, Dr. Martin B. Weimann, and Mr. Enhua Yang for various contributions.

REFERENCES

[1] Li, V.C., "From micromechanics to structural engineering--the design of cementitious Composites for civil engineering applications", *JSCE J. of Struc. Mechanics and Earthquake Engineering*, **10** (2) (1993) 37-48.

[2] Li, V.C., "Reflections on the research and development of engineered cementitious composites (ECC)," Proceedings of the JCI International Workshop on Ductile Fiber Reinforced Cementitious Composites (DFRCC) - Application and Evaluation (DRFCC-2002), Takayama, Japan, Oct., 2002, 1-21.

[3] Wang, K., Jansen, D.C., and Shah, S.P., "Permeability study of cracked concrete," *Cement and Concrete Research*, **27** (3) (1997) 381-393.

[4] Wang, S., "Micromechanics based matrix design for engineered cementitious composites," Ph.D. thesis, University of Michigan, 2005.

[5] Jensen, O. M. and Hansen, P. F., "Autogenous deformation and RH-change in perspective, *Cement and Concrete Research*, **31** (12) (2001) 1859-1865.

[6] Jensen, O. M. and Hansen, P. F., "A dilatometer for measuring autogenous deformation in hardening portland cement paste," *Materials and Structures*, **28** (181) (1995) 406-409.

[7] Lura, P., "Autogenous deformation and internal curing of concrete,' Ph. D. Thesis, Technique University of Delft, 2003.

[8] Shah, S. P., Karagular, M. E., and Sarigaphuti, M., 'Effect of shrinkage-reducing admixtures on restrained shrinkage cracking of concrete,' *ACI Materials Journal*, **89** (5) (1992) 289-295.

[9] Weimann, M. B. and Li, V. C., "Hygral behavior of engineered cementitious composites (ECC)," *International Journal for Restoration of Buildings and Monuments*, **9** (5) (2003) 513-534.